line theory, predicts the return-loss improvement obtained by using the network with a reflective antenna. The network is placed in the context of previous work by Dicke.

ACKNOWLEDGMENT

The author is indebted to the National Astronomy & Ionosphere Center (NAIC), Arecibo Observatory, Arecibo, PR, for time and facilities to develop the turnstile network. Cornell University operates NAIC under a cooperative agreement with the National Science Foundation.

REFERENCES

[1] C. G. Montgomery, R. H. Dicke, and E. M. Purcell, "Principles of microwave circuits," *Radiation Lab. Series*, vol. 8, pp. 459–466, 1948.

[2] G. L. Ragan, "Microwave transmission circuits," *Radiation Lab. Series*, vol. 9, pp. 375–377, 1948.

[3] M. A. Meyer and H. B. Goldberg, "Applications of the turnstile junction," *IRE Trans. Microwave Theory Tech.*, vol. MTT-3, pp. 40–45, Dec. 1955.

[4] R. H. Dicke, "Turnstile junction for producing circularly polarized waves," U.S. Patent 2 686 901, Aug. 17, 1954.

[5] R. K. Zimmerman, Jr., "Resonant disk turnstile," *IEEE Trans. Microwave Theory Tech.*, vol. 45, pp. 1600–1610, Sept. 1997.

A Simple Method for Blocking Parasitic Modes in a Waveguide-Packaged Microstrip-Line Circuit

Hao-Hui Chen, Chun-Long Wang, and Shyh-Jong Chung

***Abstract*— A simple structure formed by two metal patches symmetrically deposited at the two sides of the center microstrip is proposed and analyzed for blocking the higher order modes in a waveguide-packaged microstrip-line circuit. The variations (with the patch width) of the effective dielectric constants and field distributions of the modes in the packaged microstrip line with infinitely long side patches were first investigated using the two-dimensional (2-D) finite-element method (FEM) and the method of lines. The results suggested that there exists a range of patch widths at which the field distributions of the higher order modes are totally different from those of the microstrip line without side patches. The scattering of the patches as a function of the patch length and width was then studied using the three-dimensional (3-D) FEM with edge elements. It has been found that by simply choosing appropriate patch sizes, the parasitic higher order mode can be reflected without sacrificing the normal propagation of the dominant mode.**

***Index Terms*— Finite-element method, packaged microstrip line, side patches, spurious modes.**

I. INTRODUCTION

Microwave and millimeter-wave circuits are usually shielded by a rectangular waveguide to prevent the circuits from mechanical destructions and electromagnetic interferences (EMI's) from the environment. As the level of the integration and/or the operation frequency increases, parasitic fields may be excited by active devices and/or discontinuities in the circuits and propagate in the form of the higher order modes of the shielded transmission line. When the signals (which are carried by the dominant mode) and the parasitic propagation modes travel from one circuit element toward another one, the power coupling between modes would be caused through the latter circuit element and, thus, disturbs the total circuit operation.

Manuscript received June 25, 1997; revised July 14, 1998. This work was supported by the National Science Council of the R.O.C. under Grant NSC 85-2213-E-009-001.

The authors are with the Department of Communication Engineering, National Chiao Tung University, Hsinchu 30039, Taiwan, R.O.C. (e-mail: sjchnug@cm.nctu.edu.tw).

Publisher Item Identifier S 0018-9480(98)09034-6.

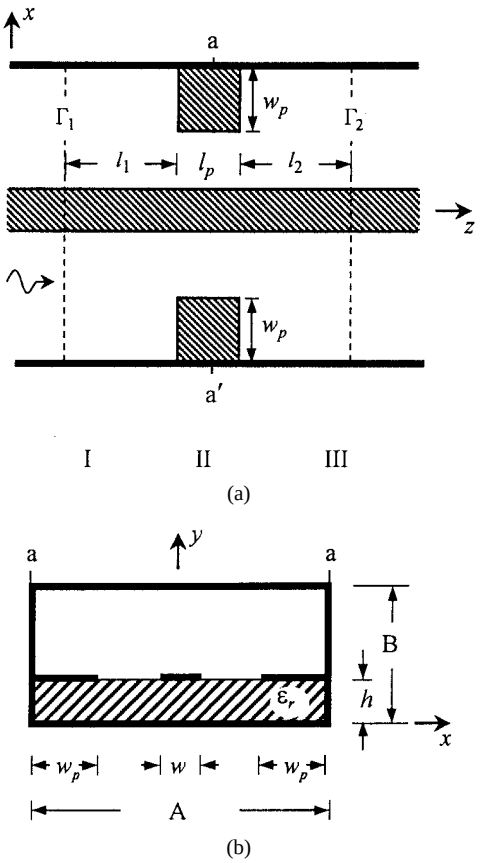

Fig. 1. A waveguide-packaged microstrip line with metal patches deposited at the two sides of the center microstrip.

To relieve the circuit element from the EMI caused by the parasitic modes, several possible approaches can be found in [1]–[5]. Deforming the enclosures or using anisotropic substrates can increase the cutoff frequencies of the higher order modes in a packaged microstrip line or a coplanar waveguide [1], [2]. Placing attenuating elements (such as resistive films and microwave absorbers) at appropriate locations can damp the parasitic fields and package resonances [3], [4]. Also, attaching metal diaphragms can reflect the incident higher order modes [5]. Although these designs would reduce the influences of the parasitic waves on the circuit, the constructions of the structures still seemed complicated.

In this paper, we propose a simple design for blocking the higher order modes in a packaged microstrip line. As shown in Fig. 1, this method uses two side metal patches to reflect the incident parasitic modes. The patches are to be etched on the substrate at the same time as the fabrication of the microstrip-line circuit, thus making the design easily realized. In the patch-deposited microstrip-line region, since the dominant mode has most of its field concentrated in the

substrate region beneath the microstrip, the influence of the patches on this mode would be very slight unless the patches are close to the microstrip. On the other hand, the fields of the higher order modes are distributed all over the cross section of the waveguide. The patches would then deform the field distributions, resulting in a high reflectivity for the incidences of the higher order propagating modes.

II. Analysis

Fig. 1 shows the structure to be analyzed, where two identical metal patches of widths w_p and lengths l_p are symmetrically deposited at the two sides of the center microstrip. The waveguide sections without patches are denoted as waveguides I and III, and the one with patches is waveguide II. Let a propagation mode of the packaged microstrip line be incident from the left side (waveguide I) toward the patch region. This mode may be the dominant (microstrip-line) mode or a parasitic higher order propagation mode produced from some circuit element on the left-hand side of the patches. (It is noticed that although evanescent modes may also be excited by the circuit element, they can be ignored due to the fast decaying of the fields, provided that the patches are not too close to the circuit element.)

Before analyzing the scattering effects of the patches, we first calculate and compare the propagation eigenmodes of waveguide I and those of waveguide II by using the two-dimensional (2-D) finite-element method (FEM). Following the procedure of the FEM, a generalized eigenvalue problem is obtained as follows:

$$(\overline{\overline{\mathbf{A}}} + \varepsilon_{\text{eff}}\overline{\overline{\mathbf{B}}})\overline{e}_t = 0 \tag{1}$$

where $\overline{e}_t$ is an unknown vector representing the transverse components of the modal electric field and ε_{eff} is the effective dielectric constant of the corresponding mode. $\overline{\overline{\mathbf{A}}}$ and $\overline{\overline{\mathbf{B}}}$ are two matrices associated with the waveguide parameters. From this eigenvalue equation, the effective dielectric constants and field distributions for the propagation modes of waveguides I and II can then be explicitly calculated.

After the propagating eigenmodes of waveguides I and II are found, the three-dimensional (3-D) FEM with edge elements [6] is then adopted to analyze the scattering effect of the patches. Let the kth propagation mode of waveguide I be incident from the left, a system equation can then be derived as follows:

$$\overline{\overline{\mathbf{P}}}\begin{bmatrix}\overline{\mathbf{E}}_{t1}\\ \overline{\mathbf{E}}_{t2}\end{bmatrix} = \begin{bmatrix}\overline{\mathbf{S}}_k\\ 0\end{bmatrix} \tag{2}$$

where $\overline{\mathbf{E}}_{ti}$ are the unknown tangential electric fields on the FEM boundary $\Gamma_i (i = 1, 2)$, and $\overline{\mathbf{S}}_k$ is the vector associated with the incident wave. With these tangential fields being solved, the reflection and transmission of each mode in waveguides I and III are then determined [6]. It is noticed that since the fields at Γ_1 and Γ_2 are expanded only by the propagation modes, the distances between the boundaries and patches, i.e., l_1 and l_2, should be large enough to reduce the error caused by ignoring the evanescent modes. For minimizing the required computation time and memories, the boundary-marching method [7] is used to handle these large regions.

III. Results and Discussions

In this paper, we set $h = w = 0.635$ mm, $\varepsilon_r = 9.7$, the packaging waveguide sizes $A \times B = 10h \times 4h$, and the frequency $f = 25$ GHz. Under this choice of parameters, there are two propagation modes, i.e., the dominant mode and second-order mode, existing in waveguide I. It is noticed that these two modes are both even modes.

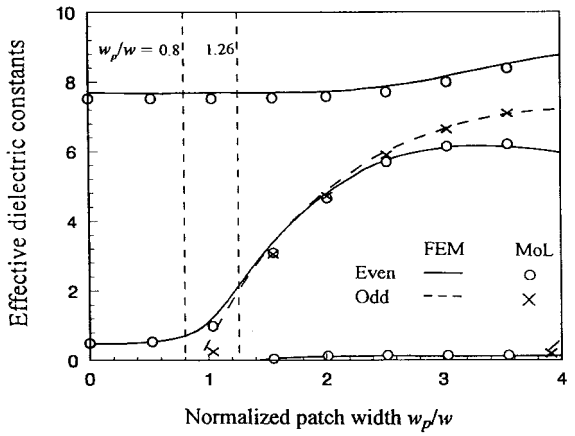

Fig. 2. The variations of the effective dielectric constants, as a function of the normalized patch width (w_p/w). $A \times B = 10h \times 4h$, $f = 25$ GHz. The solid and dash lines represent the even and odd modes calculated using the FEM, while the circles and crosses represent those calculated using the method of lines.

We first investigated the characteristics of the propagation modes in waveguide II. Fig. 2 presents the variations of the effective dielectric constants of the propagation modes as functions of the patch width. It is seen that the dominant mode is affected by the patches very slightly as long as the patch width is less than $2.5w$. However, the influence caused by the patches is apparent for the higher order modes. The effective dielectric constants of the second-order mode first increases and then slightly decreases with the raise of w_p, and the first odd and third even modes change from evanescent modes to propagation ones when the patch width is larger than $0.9w$ and $1.45w$, respectively. (For convenience, the last two modes are numbered as the third-order (first odd) and fourth-order (third even) modes in the following.) It is noticed that when $w_p > 0.9w$, the effective dielectric constants of the second- and third-order modes increase rapidly as the increase of w_p, and these two modes become degenerate at about $w_p = 1.15w$. On the contrary, the fourth-order mode has an effective dielectric constants approaching a stable value (about 0.1) as w_p increases beyond $1.6w$. As a numerical check, the results calculated from the method of lines [8] are also presented in the figure. Good agreement is observed between the results of the two methods.

Since the propagation of a mode from waveguides I to III relies on the similarity of the field distributions between this mode and those of the modes in waveguide II, we examine the patch effect on the modal power distributions of the modes in waveguide II. (Note that the modal power distribution is proportional to the square of the modal tangential electric (or magnetic) field.) Fig. 3(a)–(c) presents the power distributions of the second-order modes for, respectively, $w_p = 0$ (no patches, i.e., waveguide I), $0.8w$, and $1.26w$ (referring to Fig. 2). For $w_p = 0$, the power of the second-order mode is mainly distributed over the region above the microstrip [see Fig. 3(a)]. When patches of small width ($w_p = 0.8w$) are deposited, although part of the power is shifted to the regions around the patches, most of the power is still concentrated above the microstrip [see Fig. 3(b)]. However, when the patch width is further increased to $1.26w$, where the third-order mode has been produced and degenerates with the second-order mode, most of the second-order-mode power is shifted to the regions beneath the patches, as shown in Fig. 3(c). The large variation of the power distribution would reduce the power transfer between the present mode and second-order mode of waveguide I. When the patch width is further increased to $2w$, the fourth-order mode has been generated. Although not shown here, the power distribution of the second-order mode is similar to that

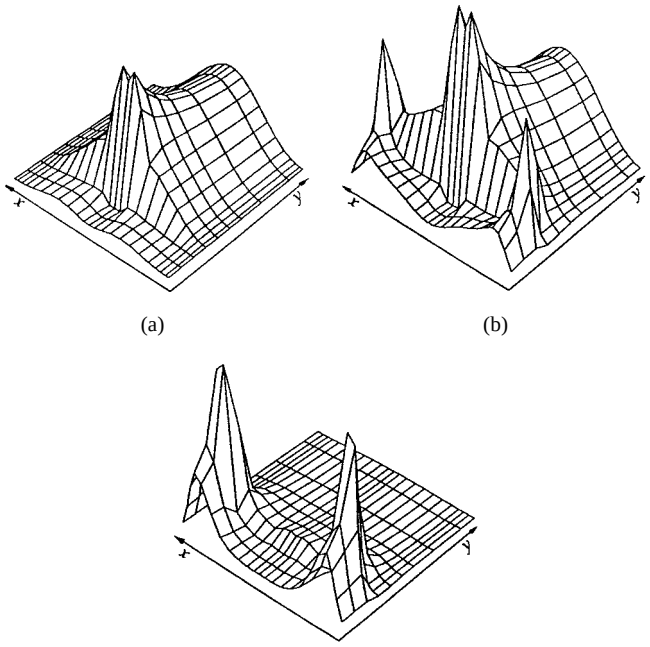

Fig. 3. The modal power distribution of the second-order mode for (a) $w_p = 0$, (b) $w_p = 0.8w$, and (c) $w_p = 1.26w$. $A \times B = 10h \times 4h$, $f = 25$ GHz.

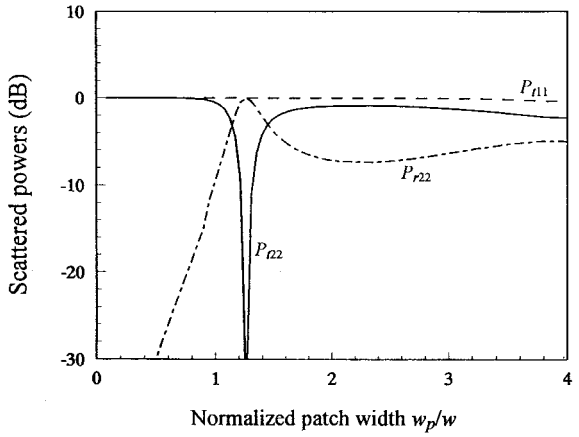

Fig. 4. The scattering effect of the patches on the propagation modes as a function of the normalized patch width (w_p/w). $l_p = 2.4w$, $A \times B = 10h \times 4h$, $f = 25$ GHz.

of $w_p = 1.26w$ [see Fig. 3(c)], with more power concentrated in the patch areas. However, the fourth-order mode possesses a power distribution quite like that of the second-order mode of waveguide I [see Fig. 3(a)]. With this patch width, the power of an incident second-order mode from waveguide I can, thus, be greatly coupled to waveguide II (and thus, waveguide III) through this fourth-order mode. The power distributions of the dominant mode at the above four patch widths have been examined to be approximately the same.

Fig. 4 shows the variations of the scattering effects of patches, as functions of the patch width. The patch length l_p is set to be $2.4w$. $P_{tij}(P_{rij})$ represents the transmitted (reflected) power of the ith mode in waveguide III (I) due to the incidence of jth mode from waveguide I. It is seen that P_{t11} remains constant over the considered range of w_p (especially in the range of $w_p < 2.5w$), which means that the transmission of the dominant mode is not influenced by the patches. However, for the second-order-mode incidence,

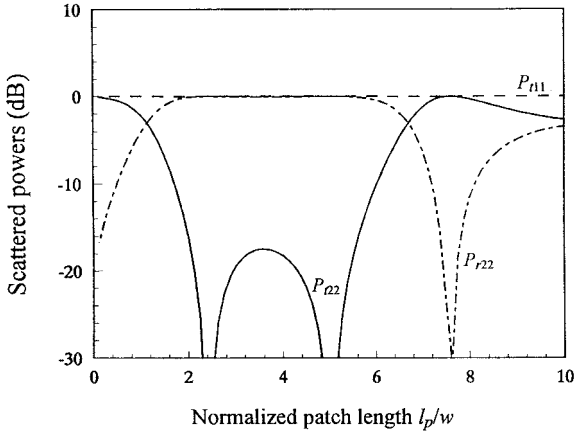

Fig. 5. The scattering effect of the patches on the propagation modes as a function of the normalized patch length (l_p/w). $w_p = 1.26w$, $A \times B = 10h \times 4h$, $f = 25$ GHz.

large variations of the transmission (P_{t22}) and reflection (P_{r22}) are observed. A low transmission of the second-order mode can be obtained in the range of $1.15w < w_p < 1.6w$, where the second- and third-order modes in waveguide II are degenerate and the fourth-order mode is unstable (i.e., the effect dielectric constant varies seriously with the increase of w_p). In this range, the modal field distributions of these modes are quite different from that of the incident second-order mode (see Fig. 3). It is noticed that at $w_p = 1.26w$, the incident power is totally reflected back to waveguide I ($P_{r22} \approx 0$ dB). The power transmitted to waveguide III (P_{t22}) is only -37 dB. Although not shown here, it has been found that the powers coupled to the dominant mode (i.e., P_{r12} and P_{t12}) are about -30 dB in the range of $1.15w < w_p < 1.6w$.

Finally, Fig. 5 displays the influence of the patch length l_p on the scattering effect of the patches. As can be seen, the increase of the patch length does not influence the propagation of the dominant mode (P_{t11}), but, due to the bouncing of the excited second-order mode in waveguide II, would vary the scattering effect for the second-order-mode incidence. In the range of $2w < l_p < 5.6w$, the reflected power P_{r22} is about 0 dB and the power (P_{t22}) leaked to waveguide III is less than -18 dB. Two minimum values of P_{t22} are obtained at $l_p = 2.4w$ ($P_{t22} = -37$ dB) and $5.0w$ ($P_{t22} = -50$ dB). With these two patch lengths, the patches can provide the best blocking effect to the incident second-order mode without sacrificing the normal propagation of the dominant mode.

IV. Conclusions

We have proposed a simple method (i.e., depositing metal patches at two sides of the center microstrip) for blocking the parasitic waves in a waveguide-packaged microstrip line circuit. From the 2-D FEM analysis, it has been found that there exists a range of patch widths where the field distributions of the higher order modes are quite different from those in the waveguide without patches so that the power couplings can be reduced. The 3-D FEM analysis has also ensured the existence of this range. The results have shown that with appropriate design, the side patches can totally reflect the incident second-order mode, while have little influence on the propagation of the dominant mode.

References

[1] R. K. Hoffmann, *Handbook of Microwave Integrated Circuits.* Norwood, MA: Artech House, 1987, pp. 399–400.

[2] A. C. Polycarpou, M. R. Lyons, and C. A. Balanis, "Finite element analysis of MMIC waveguide structures with anisotropic substrates," *IEEE Trans. Microwave Theory Tech.*, vol. 44, pp. 1650–1663, Oct. 1996.
[3] P. Mezzanotte, M. Mongiardo, L. Roselli, R. Sorrentino, and W. Heinrich, "Analysis of packaged microwave integrated circuits by FDTD," *IEEE Trans. Microwave Theory Tech.*, vol. 42, pp. 1796–1801, Sept. 1994.
[4] S. J. Chung and L. K. Wu, "Analysis of the effects of a resistively coated upper dielectric layer on the propagation characteristics of hybrid modes in a waveguide shielded microstrip using method of lines," *IEEE Trans. Microwave Theory Tech.*, vol. MTT-41, pp. 1393–1399, May 1993.
[5] H. H. Chen and S. J. Chung, "Shielding effect of a diaphragm in a packaged microstrip circuit," *IEEE Trans. Microwave Theory Tech.*, vol. 43, pp. 1082–1086, May 1995.
[6] J. Jin, *The Finite Element Method in Electromagnetics.* New York: Wiley, 1993.
[7] S. L. Foo and P. P. Silvester, "Boundary-marching method for discontinuity analysis in waveguides of arbitrary cross section," *IEEE Trans. Microwave Theory Tech.*, vol. 40, pp. 1889–1893, Oct. 1992.
[8] R. Pregla and W. Pascher, "The method of lines," in *Numerical Techniques for Microwave and Millimeter Wave Passive Structures*, T. Ithoh, Ed. New York: Wiley, 1989, ch. 6.

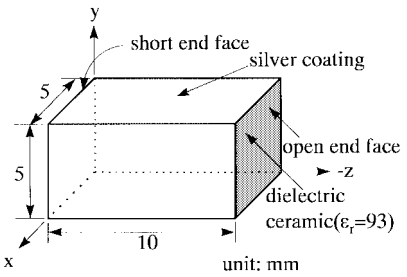

Fig. 1. Structure of the dual-mode $\lambda/4$ resonator.

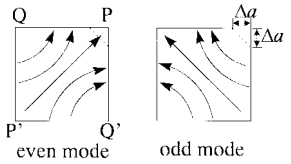

Fig. 2. Two basis modes for estimation of coupling.

Equivalent-Circuit Representation and Explanation of Attenuation Poles of a Dual-Mode Dielectric-Resonator Bandpass Filter

Ikuo Awai, Arun C. Kundu, and Takeharu Yamashita

***Abstract*— A $\lambda/4$ rectangular-waveguide resonator of square cross section filled with high-permittivity ceramics has two degenerate lowest modes. A dual-mode bandpass filter based on this structure is studied, focusing on the attenuation poles at both sides of the passband. It is described how to achieve capacitive and inductive coupling between dominant modes of a resonator of square cross section. An equivalent-circuit model is proposed, including mode coupling, excitation from the external circuit, and direct coupling between input/output (I/O) electrodes. Equivalent-circuit parameters are measured and their validity is verified using simulated result. Appearance and annihilation of the attenuation poles are successfully explained by the proposed model, and attenuation pole frequencies are controlled by shifting the I/O electrode transversely.**

***Index Terms*—Attenuation pole, dielectric resonator, dual mode, equivalent circuit.**

I. Introduction

Dual-mode resonators are one of the most effective means for miniaturizing a bandpass filter (BPF). Hence, many studies have contributed to elucidate the mechanism of coupling between dual modes and principles of fabricating a BPF [1], [2]. Attenuation poles outside of the passband, on the other hand, help to improve the skirt characteristics, resulting in further miniaturization of a BPF through reduction of the number of resonators. Though an equivalent-circuit model of an electromagnetic structure is valid only in a narrow band, it is easier to understand and gives a clear insight into the physics of the object. Thus, we will try to show the origin of attenuation poles that appear in a dual-mode two-stage BPF and try to control them based on an equivalent circuit.

The attenuation poles of a dual-mode cavity filter was explained by Zaki *et al*. [3] in an intelligible manner. However, our current work is an improved one from the following point of view: the configuration is simpler for excitation, tuning, and coupling of dual-modes, and also for the second coupling path that is essential to attenuation poles. Both types of excitation (capacitive and inductive) are possible here. Our lumped-element equivalent circuits are intuitively understandable, and the equivalent-circuit parameters are readily determined.

Manuscript received November 24, 1997; revised August 10, 1998.

The authors are with the Department of Electrical and Electronic Engineering, Yamaguchi University, Ube 755, Japan.

Publisher Item Identifier S 0018-9480(98)09051-6.

II. Coupling Between Dual Degenerate Modes

The physical structure of a directly silver-coated $\lambda/4$ dielectric waveguide resonator of square cross section, having a dimension of 5 mm × 5 mm × 10 mm, is shown in Fig. 1, where the dual modes are named as TE'_{101} and TE'_{011} [4]. We will now define new basis modes by vectorial addition and subtraction of TE'_{101} and TE'_{011} modes, naming them even and odd modes, respectively, as shown in Fig. 2.

If we add a triangular metal pattern at the corner of the OEF [2], it will make an additional current path to the resonant modes, resulting in a frequency shift in the basis modes. When the pattern is located at the corner P and/or P' of Fig. 2, it decreases inductance of the odd mode and, thus, increases the resonant frequency with little effect to the even-mode frequency. The coupling constant is simply

$$k = \frac{\left|f^{o2} - f^{e2}\right|}{f^{o2} + f^{e2}} \tag{1}$$

where f^e and f^o are the even- and odd-mode resonant frequency, respectively.

The coupling constant versus dimension of triangular metal pattern is shown in Fig. 3. From this figure, we observe that the coupling constant increases proportionally to the area of metal pattern. The validity and accuracy of this coupling method is confirmed by comparing the finite-difference time-domain (FDTD) analysis data with measured results.

An equivalent lumped-element circuit model for magnetic coupling i.e., inductive coupling between two parallel *LC* resonators, is illus-